Sun *et al. The Journal of Headache and Pain* (2024) 25:186
https://doi.org/10.1186/s10194-024-01896-y

The Journal of Headache and Pain

RESEARCH Open Access

# Causal relationships between cortical brain structural alterations and migraine subtypes: a bidirectional Mendelian randomization study of 2,347 neuroimaging phenotypes

Zuhao Sun[1†], Mengge Liu[1†], Guoshu Zhao[1†], Zhihui Zhang[1], Jinglei Xu[1], Linlin Song[1], Wanwan Zhang[1], Shaoying Wang[1], Linlin Jia[1], Qian Wu[1], Yue Wu[1], Haolin Wang[1], Nannan Liu[2,3*], Qian Su[4*] and Feng Liu[1*]

## Abstract

**Background** Previous studies have shown that migraines are associated with brain structural changes. However, the causal relationships between these changes and migraine, as well as its subtypes, migraine with aura (MA) and migraine without aura (MO), remain largely unclear.

**Methods** We utilized genome-wide association study (GWAS) summary statistics from European cohorts for 2,347 cortical structural magnetic resonance imaging (MRI) phenotypes, derived from both T1-weighted and diffusion tensor imaging scans ($n = 36{,}663$), with migraine and its subtypes ($n = 147{,}970$–$375{,}752$). Cortical phenotypes included both macrostructural (e.g., cortical thickness, surface area) and microstructural (e.g., fractional anisotropy, mean diffusivity) features. Genetic correlations were first assessed to identify significant associations, followed by bidirectional Mendelian randomization (MR) analyses to determine causal relationships between these brain phenotypes and migraine, as well as its subtypes (MA and MO). Sensitivity analyses were applied to ensure the robustness of the results.

**Results** Genetic correlation analysis identified 510 significant associations between cortical structural phenotypes and migraine across 401 distinct traits. Forward MR analysis revealed nine significant causal effects of cortical structural changes on migraine risk. Specifically, increased cortical thickness and local gyrification index in specific cortical regions were associated with a decreased risk of overall migraine, MA, and MO, while intracellular volume fraction and orientation diffusion index in specific regions increased the risk of MA and MO. Reverse MR analysis

†Zuhao Sun, Mengge Liu and Guoshu Zhao contributed equally to this work.

*Correspondence:
Nannan Liu
liunn1204@tmu.edu.cn
Qian Su
suqian@tjmuch.com
Feng Liu
fengliu@tmu.edu.cn

Full list of author information is available at the end of the article

demonstrated that MA causally increased mean diffusivity in the insular and frontal opercular cortex. Sensitivity analyses confirmed the robustness of these findings, with no evidence of horizontal pleiotropy or heterogeneity.

**Conclusion** This study identifies causal relationships between cortical neuroimaging phenotypes and migraine, highlighting potential biomarkers for migraine diagnosis, treatment, and prevention.

**Keywords** Migraine, Cortical neuroimaging, Mendelian randomization, Brain structure, Migraine subtypes

## Introduction

Migraine is a highly prevalent neurological disorder, affecting approximately 15% of the global population [1]. It is characterized by recurring episodes of moderate to severe headache, often accompanied by nausea, vomiting, and super-sensitivity to light and sound [2, 3]. Migraine is primarily categorized into two major subtypes: migraine without aura (MO) and migraine with aura (MA) [3]. MO, which is more common, is defined by headaches that are typically unilateral and pulsating, occurring without any preceding neurological symptoms [4]. In contrast, MA is characterized by similar headache features but is preceded by transient neurological symptoms, such as visual or sensory disturbances, collectively referred to as auras [5]. The different neurological symptoms of the two subtypes implied different involvement patterns of brain regions. Identification of the migraine-related brain regions would play a vital role in discovering the underlying neurobiological mechanisms, further facilitate the researches of migraine diagnosis, prevention and treatment.

Through structural magnetic resonance imaging (MRI), including both T1-weighted and diffusion tensor imaging (DTI), the brain cortex can be characterized by a variety of phenotypes, particularly macrostructural and microstructural cortical phenotypes [6, 7]. Macrostructural cortical phenotypes include measures such as cortical thickness (CT), surface area (SA), and cortical volume (CV), which provide insights into the overall architecture and size of the cerebral cortex. Microstructural cortical phenotypes, derived from diffusion MRI techniques, include metrics such as fractional anisotropy (FA) and mean diffusivity (MD), offering a detailed view of the tissue's microstructural integrity, including neural fiber organization and cellular density. Research has shown that individuals with migraines may exhibit both macrostructural and microstructural brain alterations [8–12]. For example, changes in gray matter volume have been reported, suggesting neuroanatomical differences in migraine sufferers [13–16]. Microstructural changes, such as variations in white matter integrity, have also been observed, potentially reflecting the impact of chronic pain or recurrent migraine episodes [17–20]. However, these findings primarily stem from observational studies that are limited by confounding factors and cannot establish a causal relationship. It remains unclear whether these structural changes are a cause or a consequence of migraines, or if they differ between the subtypes MO and MA, prompting the necessity for deeper exploration.

To address these challenges and better understand the potential causal relationships between migraine subtypes and brain structure, Mendelian randomization (MR) provides a robust approach [21, 22]. MR utilizes genetic variants as instrumental variables (IVs) to infer causality between an exposure (such as specific brain structural phenotypes) and an outcome (such as migraine) [22, 23]. This method exploits the random allocation of genetic variants at conception, akin to randomization in clinical trials, thereby reducing the influence of confounding factors and reverse causation. Through MR, we can investigate whether certain brain structural characteristics causally increase the risk of developing specific migraine subtypes, and conversely, whether genetic predispositions to migraines lead to particular structural changes in the brain. This dual approach provides clearer insights into the complex interplay between brain structure and migraine, potentially identifying early biomarkers for intervention and novel therapeutic targets. Several MR analyses have explored the causal relationships between brain MRI measurements and migraine. For instance, one MR study indicated that SA and hippocampal volume may be causally linked to migraine risk [24]. Another study highlighted the causal association between migraine and microstructural changes in white matter [25]. However, these studies primarily focus on a single type of migraine or a specific brain MRI phenotype, leaving the broader causal relationships between various brain MRI phenotypes and different migraine subtypes still largely unexplored.

In this study, the causal relationships between a broad set of cortical structural phenotypes and migraine, including its subtypes (MO and MA), were comprehensively explored. Genome-wide association study (GWAS) summary statistics for 2,347 cortical MRI phenotypes, derived from both T1-weighted and DTI, were utilized. Genetic correlations were first examined to identify significant associations. Bidirectional MR was then applied to assess whether cortical macrostructural and microstructural changes contributed to migraine susceptibility and, conversely, whether genetic predispositions to migraine led to cortical structural alterations. This study

provided the most extensive examination to date of the cortical structural basis of migraine and its subtypes, offering new insights into the underlying neurobiological mechanisms.

## Methods

### Data sources

#### *MRI phenotype GWAS*

In this study, we included 13 cortical brain MRI phenotypes, consisting of eight macrostructural features (i.e., CT, SA, CV, folding index [FI], intrinsic curvature index [ICI], local gyrification index [LGI], mean curvature [MC], and Gaussian curvature [GC]) and five microstructural features (i.e., FA, MD, isotropic volume fraction [ISOVF], intracellular volume fraction [ICVF], and orientation diffusion index [ODI]) [26]. The macrostructural features were derived from T1-weighted imaging, which provides high-resolution structural information about the brain, while the microstructural features were obtained from DTI, which assesses tissue microstructure. The data for these phenotypes were obtained from the UK Biobank (UKB) and the Adolescent Brain Cognitive Development (ABCD) cohorts. The brain cortex was parcellated into 180 bilaterally averaged regions using the Human Connectome Parcellation scheme (Supplementary Table 1), resulting in a total of 2,347 cortical phenotypes (Supplementary Table 2). These phenotypes included 13 global phenotypes and 2,334 regional phenotypes (calculated as 13 phenotypes across 180 regions, minus 6 phenotypes that exhibited no variance). For all 2,347 cortical MRI phenotypes, raw measurements were standardized to a mean of zero and a standard deviation of one. A linear mixed-effects model was used for the MRI phenotype GWAS, controlling for age, age$^2$, sex, age × sex, age$^2$ × sex, imaging center, the top 40 genetic principal components, mean framewise displacement, maximum framewise displacement, and Euler Index. The GWAS was conducted separately for the UKB (31,797 participants, median age 64) and ABCD (4,866 participants, median age 10) cohorts, and the results were combined using an inverse variance-weighted meta-analysis, resulting in a total of 36,663 European individuals. For more information about the MRI phenotypes, please refer to the details provided in the Supplementary Text.

#### *Migraine GWAS*

We included three types of migraine in the present study: overall migraine (59,674 cases, 316,078 controls), MA (6,332 cases, 144,883 controls), and MO (8,348 cases, 139,622 controls) [27]. The migraine GWAS data were derived from an inverse variance-weighted meta-analysis of 22 individual GWASs conducted by the International Headache Genetics Consortium (IHGC), with cases diagnosed either by self-report or based on the second edition of the International Classification of Headache Disorders (ICHD-2) (Supplementary Table 3).

All participants in both the cortical MRI and migraine GWAS datasets were of European ancestry, with no overlap between the two datasets. Ethical approval and informed consent were obtained in the original studies.

### Genetic correlation analysis

Genetic correlations between the 7,041 cortex-migraine pairs (i.e., three migraine types × 2,347 cortical MRI phenotypes) were estimated using linkage disequilibrium score regression (LDSC) analyses, based on GWAS summary statistics [28]. Precomputed LD scores from the 1000 Genomes Project European population were used, with the analyses restricted to HapMap3 single nucleotide polymorphisms (SNPs). Cortex-migraine pairs with a genetic correlation *P*-value of less than 0.05 were considered significant and selected for subsequent MR analyses.

### MR analysis

Genetic variants were used as IVs to estimate the causal relationships between cortical MRI phenotypes and migraine through a bidirectional MR framework. For the IVs to be valid, they needed to meet three key assumptions: strong association with the exposure, independence from confounders, and an exclusive effect on the outcome through the exposure. In this study, IVs (i.e., SNPs) were selected using a significance threshold of $P<1\times10^{-5}$ to ensure adequate strength across all exposures, a threshold frequently used in other MR studies [29–31]. Independent IVs were then identified through linkage disequilibrium (LD) clumping, with a window size of 10,000 kb and an LD threshold of $r^2 < 0.001$, ensuring that selected IVs were not in high LD with one another. Next, the effect alleles of the IVs were harmonized between the exposure and outcome datasets using the *harmonise_data()* function in the *TwoSampleMR* package, with palindromic IVs having minor allele frequencies greater than 0.42 excluded to avoid strand ambiguity, a threshold that is a built-in parameter in the default setting. After that, Steiger filtering was applied to remove IVs showing stronger associations with the outcome than the exposure, thereby addressing potential reverse causality [32]. Outliers were subsequently identified and excluded using RadialMR [33]. Finally, *F*-statistics were calculated for the retained IVs, with an *F*-statistic greater than 10 indicating sufficient strength to minimize the risk of weak instrument bias [34].

A bidirectional MR approach was employed to investigate the causal relationships between cortical MRI phenotypes and migraine. The forward MR analysis assessed the causal effects of cortical MRI phenotypes on migraine and its subtypes, while the reverse MR analysis evaluated the impact of migraine and its subtypes on cortical

MRI traits. The inverse variance weighted (IVW) method was selected as the primary approach for both forward and reverse MR analyses, as it provides the most efficient causal estimates under the assumption that all IVs are valid, offering the greatest statistical power [35]. To mitigate potential bias from invalid IVs, several additional MR methods were applied, including the robust adjusted profile score (MR-RAPS) [36], weighted median, weighted mode, and MR-Egger methods. MR-RAPS is particularly useful for handling weak instrument bias by adjusting the profile likelihood of summary data. The weighted median method delivers reliable causal estimates even if up to 50% of IVs are invalid, while the weighted mode method is resilient to outliers, assuming the majority of IVs are valid. MR-Egger accounts for pleiotropic effects and can provide consistent causal estimates under the assumption of a weaker instrument strength independent of direct effects. Both forward and reverse MR-IVW results were adjusted for multiple comparisons using false discovery rate (FDR) correction. A causal relationship was deemed significant if the MR-IVW estimate had an FDR-corrected $P<0.05$ and its effect direction was consistent with those of the other MR methods. All MR analyses were conducted using the *TwoSampleMR* package (version 0.6.6) in *R* (version 4.3.3).

Sensitivity analyses were conducted to assess potential violations of MR assumptions. First, the MR-Egger intercept test was used to detect directional pleiotropy, indicating whether invalid IVs introduced bias. Second, heterogeneity among IVs was evaluated using Cochran's *Q* test for MR-IVW and Rucker's *Q* test for MR-Egger, providing insight into variability across IVs [37]. Third, MR-PRESSO was applied to identify and correct for potential outliers that could influence causal estimates. Finally, MR plots were generated for visual inspection of heterogeneity and pleiotropy. Specifically, a leave-one-out plot was used to determine if the MR-IVW estimates were driven by specific IVs with strong effects. A forest plot displayed the individual effects of each IV, while a scatter plot illustrated the alignment of MR estimates across all IVs. A funnel plot depicted the distribution of effect sizes, allowing for further examination of pleiotropic bias.

## Results

### Genetic correlations

LDSC analyses were performed to evaluate genetic correlations between 2,347 cortical MRI phenotypes and three migraine types: overall migraine, MA, and MO, leading to a total of 7,041 cortex-migraine pairs. Of these, 510 nominally significant genetic correlations were identified, spanning 401 distinct cortical MRI phenotypes (Fig. 1, Supplementary Table 4). Overall migraine was correlated with 179 cortical phenotypes, with correlation coefficients ranging from −0.22 to 0.28. MA exhibited correlations with 148 cortical phenotypes, with coefficients ranging from −0.52 to 0.48, while MO was associated with 183 cortical phenotypes, with coefficients ranging from −0.36 to 0.46 (Fig. 2, Supplementary Table 4).

Additionally, distinct patterns of association were observed across the different migraine types (Fig. 2, Supplementary Table 4). Overall migraine was mainly linked to CV in 36 regions, LGI in 20 regions, and GC in 20 regions. MA was predominantly correlated with ICVF in 69 regions, while MO displayed only one correlation with ICVF. Conversely, MO showed stronger associations with SA, with significant correlations in 50 regions, whereas MA was associated with SA in only one region. These findings suggest that each migraine type has distinct genetic correlation patterns with various cortical structural phenotypes, providing a foundation for further causal investigation using MR.

### MR results

All the IVs for MR were listed in Supplementary Table 5. In the forward MR analysis, nine significant causal effects of cortical MRI phenotypes on the risk of migraine and its subtypes were identified (FDR-corrected $P<0.05$) (Fig. 3, Supplementary Table 6). For overall migraine, three cortical phenotypes were associated with a decreased risk: increased CT in the anterior cingulate and medial prefrontal cortex, specifically in area posterior 24, was associated with a lower risk, with an OR of 0.85 (95% CI=0.77–0.93, $P=7.82\times10^{-4}$). Similarly, the LGI in the anterior cingulate cortex (area 10v) showed a reduced risk (OR=0.87, 95% CI=0.81–0.95, $P=7.09\times10^{-4}$), and the CV in area posterior 24 was also associated with a decreased risk of overall migraine (OR=0.81, 95% CI=0.74–0.89, $P=8.76\times10^{-6}$). For MA, increased CT in area posterior 24 was linked to a decreased risk (OR=0.62, 95% CI=0.51–0.76, $P=2.62\times10^{-6}$), while the ICVF in the insular and frontal opercular cortex (frontal opercular area 4) was associated with an increased risk of MA (OR=1.50, 95% CI=1.20–1.88, $P=3.75\times10^{-4}$). Additionally, the ICVF in the auditory association cortex (area STSd anterior) was linked to a higher risk (OR=1.33, 95% CI=1.12–1.57, $P=8.16\times10^{-4}$). For MO, a reduced ICI in the anterior cingulate and medial prefrontal cortex (area 9 middle) was associated with a decreased risk (OR=0.60, 95% CI=0.46–0.79, $P=2.37\times10^{-4}$), while the LGI in the lateral temporal cortex (area TG dorsal) showed a reduced risk of MO (OR=0.79, 95% CI=0.68–0.91, $P=8.62\times10^{-4}$). In contrast, the ODI in the inferior frontal cortex (area IFSp) was associated with an increased risk of MO (OR=1.69, 95% CI=1.35–2.10, $P=3.54\times10^{-6}$). In the reverse MR analysis, MA was found to causally increase MD in the insular and

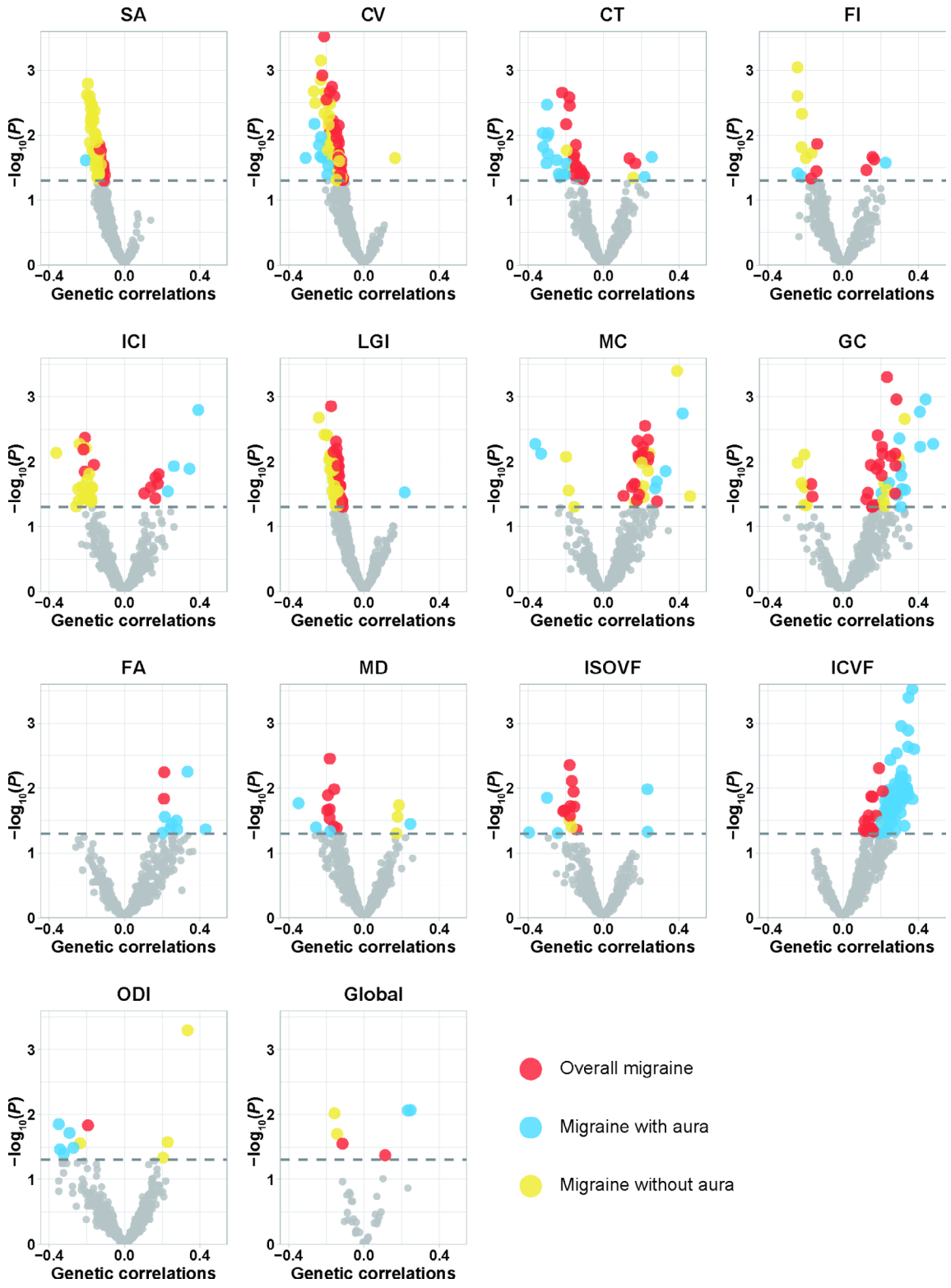


**Fig. 1** Significant genetic correlations of cortical MRI phenotypes with migraine and its subtypes. Each panel shows the genetic correlations for a specific cortical MRI phenotype with overall migraine, migraine with aura, and migraine without aura. The gray dots represent non-significant correlations. Detailed results are provided in Supplementary Table 4. Abbreviations: CT, cortical thickness; CV, cortical volume; FA, fractional anisotropy; FI, folding index; GC, Gaussian curvature; ICI, intrinsic curvature index; ICVF, intracellular volume fraction; ISOVF, isotropic volume fraction; LGI, local gyrification index; MC, mean curvature; MD, mean diffusivity; ODI, orientation diffusion index; SA, surface area

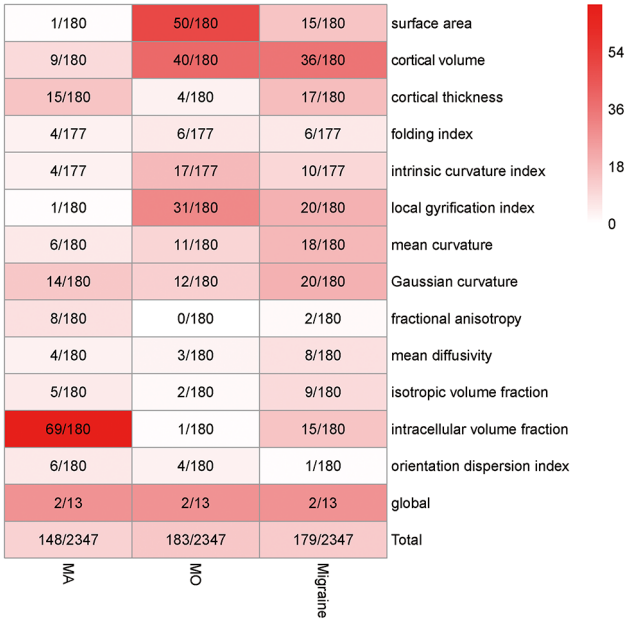


**Fig. 2** Heatmap of genetic correlations of the 2,347 cortical MRI phenotypes with migraine and its subtypes. The x-axis lists the migraine and its subtypes, while the y-axis lists the 13 kinds of reginal MRI phenotypes, one kind of global measurement, and a summary of total cortical MRI phenotypes. The color filling the cells indicates the number of significant ($P<0.05$) correlations, with the deeper red representing more significant numbers. The characters in each cell are a combination of numbers of significant and all correlations. Detailed results are presented in Supplementary Table 4. Abbreviations: MA, migraine with aura; MO, migraine without aura

frontal opercular cortex, specifically in the piriform cortex (Beta$=3.92\times10^{-4}$, SE$=9.99\times10^{-5}$, $P=8.90\times10^{-5}$) (Table 1, Supplementary Table 7).

Several sensitivity analyses were performed to assess the robustness of the MR findings (Table 2, Supplementary Table 8). The MR-Egger intercept test did not detect any evidence of directional pleiotropy across the analyses ($P>0.05$), suggesting that the IVs used in the analysis were not subject to significant horizontal pleiotropy. Additionally, Cochran's $Q$ test for MR-IVW and Rucker's $Q$ test for MR-Egger showed no significant heterogeneity among the IVs ($P>0.05$), indicating consistency in the effects across the IVs. The MR-PRESSO test further confirmed the absence of any significant outliers, supporting the validity of the causal estimates. Visual inspection of the MR plots, including the leave-one-out plot, confirmed that the results were not driven by any single IV, and the forest plot demonstrated consistent effects across individual variants (Figures S1-S10). The scatter plot showed alignment between the MR estimates and the IVs, while the funnel plot revealed a symmetrical distribution of effect sizes, providing no evidence of pleiotropic bias (Figures S1-S10). Furthermore, all $F$-statistics for the significant causal relationships were greater than 10, indicating that the instruments used were sufficiently strong to avoid weak instrument bias.

## Discussion

To our knowledge, this study represents the first comprehensive bidirectional MR analysis to explore the causal relationships between migraine, including its subtypes MA and MO, and over 2,000 cortical structural phenotypes, derived from both T1-weighted and diffusion MRI data. In forward MR analysis, we identified significant associations between both macrostructural and microstructural cortical features and migraine risk. Specifically, increased CT and LGI were associated with a decreased risk of overall migraine, MA, and MO, while certain microstructural features, such as ICVF and ODI, were linked to increased migraine susceptibility. In reverse MR analysis, MA was found to causally increase MD in the insular and frontal opercular cortex. These findings provide important insights into the neurobiological mechanisms underlying migraine, offering potential implications for diagnosis and treatment strategies.

Our LDSC analyses identified 510 significant genetic correlations between cortical MRI phenotypes and migraine, with specific MRI traits showing sensitivity to different migraine subtypes. Previous studies mainly focused on conventional brain structure measurements like CV, CT, and SA. For example, reduced CT in the precentral, pericalcarine, and temporal cortices has been observed during MO compared to interictal periods [14], while CV reduction in the subgenual anterior cingulate cortex and SA alterations in the insula and caudal anterior cingulate have been linked to MO [38, 39]. Our genetic correlation results align with these findings, showing that MO is primarily correlated with SA and CV. However, MA displayed a distinct pattern, being more closely associated with ICVF, which reflects the fraction of tissue made up of neurites [26]. This difference highlights the varying neurobiological mechanisms between MA and MO. Overall migraine correlations largely mirrored those of MO, which is expected as MO is the predominant subtype [2]. Importantly, some MRI phenotypes correlated with MA and MO but not overall migraine, highlighting the need to consider migraine subtypes separately in research to avoid overlooking subtype-specific factors.

The results of the MR analysis demonstrated causal relationships between cortical phenotypes and the risk of overall migraine as well as its subtypes, MA and MO. In the forward MR analysis, increased CT and LGI in the anterior cingulate cortex and medial prefrontal cortex were found to have a causal effect in reducing the risk of overall migraine. These regions are involved in pain processing and emotional regulation [40–42], suggesting that thicker cortices and more complex cortical folding

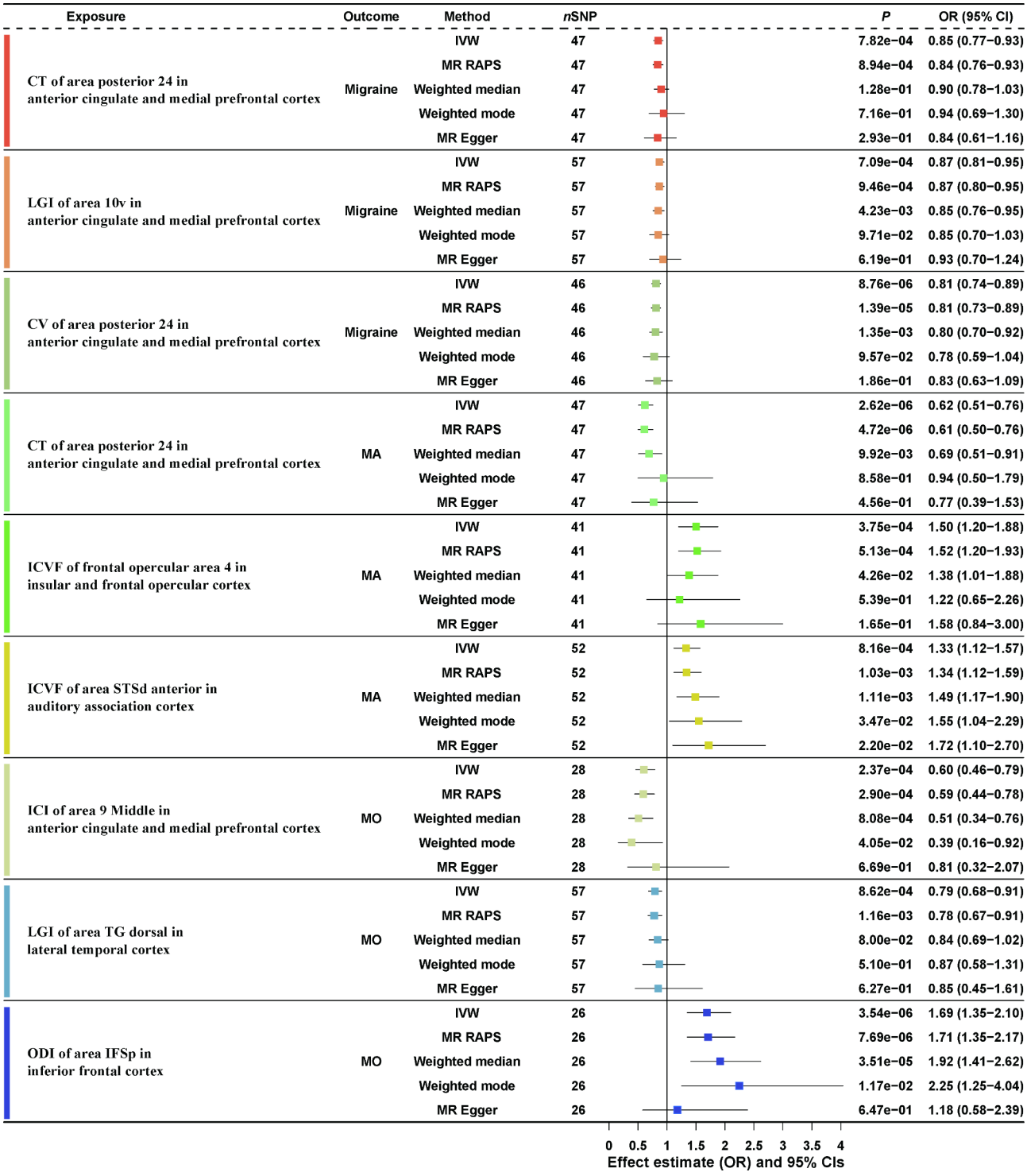


**Fig. 3** Significant causal effects of cortical MRI phenotypes on migraine and its subtypes. Full results are presented in Supplementary Table 6. Abbreviations: IVW, inverse variance weighted; MA, migraine with aura; MO, migraine without aura; RAPS, robust adjusted profile score

may provide a neuroprotective effect, reducing the likelihood of experiencing migraines by improving the brain's ability to modulate pain signals and emotional responses. For the MA subtype, the forward MR analysis identified that increased ICVF and ODI in the insular and frontal opercular cortex had a causal effect in increasing the risk of MA. These regions are critical for sensory integration and autonomic regulation [43–45], which are often disturbed during MA episodes [2, 46, 47]. The changes in microstructural properties, such as increased ICVF and

**Table 1** Significant causal effect of MA on cortical MRI phenotype

| Exposure | Outcome | Method | nSNP | Beta | SE | *P* |
|---|---|---|---|---|---|---|
| MA | MD of piriform cortex in insular and frontal opercular cortex | Inverse variance weighted | 43 | 3.92E-04 | 9.99E-05 | 8.90E-05 |
| | | MR-RAPS | 43 | 4.09E-04 | 1.07E-04 | 1.33E-04 |
| | | Weighted median | 43 | 5.04E-04 | 1.47E-04 | 5.91E-04 |
| | | Weighted mode | 43 | 5.48E-04 | 2.17E-04 | 1.98E-02 |
| | | MR Egger | 43 | 1.00E-04 | 2.00E-04 | 6.23E-01 |

Note Full results are presented in Supplementary Table 7. Abbreviations: MA, migraine with aura; MD, mean diffusivity; RAPS, robust adjusted profile score

ODI [26], suggest that alterations in cellular density and fiber organization in these areas may contribute to the heightened sensitivity and aura symptoms characteristic of MA. In the case of MO, the forward MR analysis showed that increased ODI in the inferior frontal cortex had a causal effect on increasing the risk of MO. This region is involved in cognitive control and pain regulation [48, 49], and its structural disruptions may impair the brain's capacity to manage pain signals effectively [9, 50], leading to more frequent or severe migraine attacks in individuals with MO. The reverse MR analysis provided additional insights, showing that MA had a causal effect on increasing MD in the insular and frontal opercular cortex. This suggests that recurrent MA episodes may induce progressive microstructural changes in these regions, which are essential for processing sensory input and autonomic functions.

In our MR study, we identified nine forward causal relationships and one reverse causal relationship, suggesting a bidirectional interaction between cortical structure and migraine risk. The forward relationships indicate that specific cortical structural features may reduce the risk of developing migraine, while certain microstructural alterations increase susceptibility to migraine, particularly in cases of MA. The reverse relationship suggests that migraine episodes, especially those involving aura, could influence cortical structural changes. This bidirectional interaction may indicate that alterations in the brain's structure predispose individuals to migraine, and in turn, migraine attacks—particularly those with aura—may contribute to ongoing structural changes. Alternatively, the forward and reverse causal relationships may exist in separate pathways, where cortical features influencing migraine risk serve as biomarkers, while structural changes driven by migraine represent potential targets for intervention. These results highlight the distinct neurobiological mechanisms underlying different types of migraine, with specific cortical regions and structural features playing causal roles in migraine susceptibility. Understanding these causal pathways offers potential for more targeted interventions and therapeutic strategies based on the specific cortical alterations associated with each migraine subtype.

Methodologically, this MR study leveraged large-scale GWAS data to infer causal relationships, providing important perspectives on the bidirectional interactions between cortical MRI phenotypes and migraine. However, the summary statistics we employed included participants of varying ages and both sexes, which may complicate the isolation of specific demographic factors, such as age and gender, that could influence these relationships [51, 52]. Additionally, although the GWAS summary data used in this study was limited to bilaterally averaged cortical MRI phenotypes, exploring hemisphere-specific structural differences could provide further insights into the relationship between migraine and brain asymmetry [53, 54]. Migraine is increasingly understood as a spectrum disorder, with substantial heterogeneity between subtypes such as MA and MO [2]. Future research using more refined GWAS datasets that account for distinct migraine subtypes and brain asymmetry may uncover subtype-specific mechanisms and provide a clearer understanding of the underlying neurobiological pathways. While we applied multiple MR methods to account for pleiotropy and heterogeneity, it is important to acknowledge that unmeasured confounders may still influence the observed relationships. Incorporating more comprehensive datasets that include lifestyle factors, such as smoking or alcohol consumption [55, 56], could help elucidate the broader context in which migraine impacts brain structure.

This study has several strengths, with the use of MR being a key advantage. MR provides a powerful approach to inferring causal relationships between cortical structural changes and migraine while effectively minimizing the influence of confounding factors that are common in observational studies [22, 57]. By using genetic variants as IVs, MR reduces the risk of reverse causality and confounding, offering stronger evidence that specific brain changes have a direct impact on migraine risk, rather than simply being a consequence of the condition. This methodological strength enhances the reliability and validity of the findings. Another major strength of this research lies in the rich and diverse set of neuroimaging phenotypes included in the analysis. The study goes beyond standard macrostructural measures, such as CT and LGI, by incorporating advanced microstructural features, like ICVF and ODI, derived from DTI scans. This comprehensive range of imaging phenotypes allows for a more in-depth understanding of how both large-scale

**Table 2** Sensitivity analyses for the 10 significant causal relationships estimated by bidirectional MR analyses

| Exposure | Outcome | *F* | Egger intercept test | | | Cochran's Q | | | Rucker's Q | | | MR-PRESSO | |
|---|---|---|---|---|---|---|---|---|---|---|---|---|---|
| | | | Intercept | SE | *P* | Q | df | *P* | Q | df | *P* | RSSobs | *P* |
| cortical thickness of Area posterior 24 in anterior cingulate and medial prefrontal cortex | migraine | 19.52 | 0.00 | 0.01 | 9.30E-01 | 42.19 | 46.00 | 6.33E-01 | 42.18 | 45.00 | 5.92E-01 | 52.14 | 4.70E-01 |
| cortical volume of Area posterior 24 in anterior cingulate and medial prefrontal cortex | migraine | 19.53 | 0.00 | 0.01 | 8.79E-01 | 37.07 | 45.00 | 7.94E-01 | 37.05 | 44.00 | 7.62E-01 | 45.21 | 6.50E-01 |
| local gyrification index of Area 10v in anterior cingulate and medial prefrontal cortex | migraine | 19.57 | 0.00 | 0.01 | 6.64E-01 | 41.52 | 56.00 | 9.25E-01 | 41.33 | 55.00 | 9.14E-01 | 34.92 | 9.46E-01 |
| cortical thickness of Area posterior 24 in anterior cingulate and medial prefrontal cortex | MA | 19.52 | -0.01 | 0.01 | 5.39E-01 | 37.02 | 43.00 | 7.27E-01 | 36.63 | 42.00 | 7.05E-01 | 29.51 | 9.05E-01 |
| intracellular volume fraction of Area STSd anterior in auditory association cortex | MA | 19.55 | -0.01 | 0.01 | 2.30E-01 | 43.97 | 51.00 | 7.47E-01 | 42.49 | 50.00 | 7.66E-01 | 28.05 | 8.20E-01 |
| intracellular volume fraction of Frontal Opercular Area 4 in insular and frontal opercular cortex | MA | 19.53 | 0.00 | 0.01 | 8.63E-01 | 31.20 | 40.00 | 8.39E-01 | 31.17 | 39.00 | 8.10E-01 | 33.96 | 7.67E-01 |
| intrinsic curvature of Area 9 Middle in anterior cingulate and medial prefrontal cortex | MO | 19.55 | -0.01 | 0.02 | 5.09E-01 | 26.88 | 27.00 | 4.70E-01 | 26.42 | 26.00 | 4.40E-01 | 43.78 | 1.82E-01 |
| local gyrification index of Area TG dorsal in lateral temporal cortex | MO | 19.64 | 0.00 | 0.01 | 7.97E-01 | 38.64 | 56.00 | 9.63E-01 | 38.57 | 55.00 | 9.55E-01 | 26.57 | 7.65E-01 |
| orientation diffusion index of Area IFSp in inferior frontal cortex | MO | 19.67 | 0.02 | 0.02 | 3.09E-01 | 19.65 | 25.00 | 7.65E-01 | 18.57 | 24.00 | 7.74E-01 | 30.77 | 6.54E-01 |
| MA | mean diffusivity of Pirform Cortex in insular and frontal opercular cortex | 19.69 | 0.00 | 0.00 | 1.08E-01 | 19.94 | 21.00 | 5.25E-01 | 17.11 | 20.00 | 6.46E-01 | 27.69 | 6.14E-01 |

Note Full results are presented in Supplementary Table 8. Abbreviations: MA, migraine with aura; MO, migraine without aura

brain architecture and finer microstructural properties contribute to migraine risk. Furthermore, the inclusion of migraine subtypes, specifically MA and MO, adds another layer of specificity to the findings. By distinguishing between subtypes, the study provides valuable insights into the unique neurobiological mechanisms underlying MA and MO, which could be missed in studies treating migraine as a single entity. This differentiation between subtypes strengthens the study by highlighting the distinct cortical changes associated with each form of migraine, contributing to a deeper understanding of migraine pathophysiology and offering potential avenues for targeted therapeutic interventions.

Despite the strengths of this study, several limitations should be acknowledged. First, the analysis was restricted to individuals of European ancestry, which may limit the generalizability of the findings to other populations. Further studies across diverse ancestries are necessary to validate these results. Second, the study focused exclusively on cortical structural phenotypes, without including subcortical or white matter features, which may also be relevant to migraine pathophysiology. Third, although large-scale GWAS data were employed, the study may still lack the statistical power to detect smaller genetic effects or more detailed relationships between brain structure and migraine subtypes. Fourth, the cross-sectional nature of the MRI data prevents exploration of temporal dynamics, which could offer deeper insights into migraine progression. Fifth, the inclusion of the ABCD cohort, which consists of younger participants (aged 9–10 years), may affect MRI segmentation accuracy due to ongoing brain maturation, particularly in cortical regions still developing. This could introduce variability in the results, and future studies should consider age-stratified analyses to better account for developmental differences. Finally, while Mendelian randomization reduces confounding, the possibility of unmeasured confounders cannot be entirely ruled out, potentially impacting the causal interpretations.

## Conclusions

In conclusion, this study provides robust evidence for the causal links between cortical structural phenotypes and migraine, offering new insights into the neurobiological pathways involved in both overall migraine and its subtypes. The identification of specific cortical regions associated with migraine risk, as well as the reciprocal impact of migraine on brain microstructure, underscores the complexity of these relationships. These findings not only advance our understanding of the structural brain changes linked to migraine but also highlight potential targets for future therapeutic interventions. Continued research is needed to further elucidate these mechanisms and explore their clinical applications.

**Abbreviations**

| | |
|---|---|
| ABCD | Adolescent Brain Cognitive Development |
| CT | Cortical thickness |
| CV | Cortical volume |
| FA | Fractional anisotropy |
| FDR | False discovery rate |
| FI | Folding index |
| GC | Gaussian curvature |
| GWAS | Genome-wide association study |
| ICI | Intrinsic curvature index |
| IHGC | International Headache Genetics Consortium |
| ISOVF | Isotropic volume fraction |
| IV | Instrumental variables |
| IVW | Inverse variance weighted |
| LD | Linkage disequilibrium |
| LDSC | Linkage disequilibrium score regression |
| LGI | Local gyrification index |
| MA | Migraine with aura |
| MC | Mean curvature |
| MD | Mean diffusivity |
| MO | Migraine without aura |
| MR | Mendelian randomization |
| MRI | Magnetic resonance imaging |
| ODI | Orientation diffusion index |
| SA | Surface area |
| SNP | Single nucleotide polymorphism |
| UKB | UK Biobank |

## Supplementary Information

The online version contains supplementary material available at https://doi.org/10.1186/s10194-024-01896-y.

**Supplementary Material 1: Figure S1.** MR plots for the causal effect of cortical thickness of area posterior 24 in anterior cingulate and medial prefrontal cortex on overall migraine. (A) Leave-one-out plot. (B) Forest plot. (C) Scatter plot. (D) Funnel plot.

**Supplementary Material 2: Figure S2.** MR plots for the causal effect of local gyrification index of area 10v in anterior cingulate and medial prefrontal cortex on overall migraine. A. Leave-one-out plot. B. Forest plot. C. Scatter plot. D. Funnel plot.

**Supplementary Material 3: Figure S3.** MR plots for the causal effect of volume of area posterior 24 in anterior cingulate and medial prefrontal cortex on overall migraine. A. Leave-one-out plot. B. Forest plot. C. Scatter plot. D. Funnel plot.

**Supplementary Material 4: Figure S4.** MR plots for the causal effect of cortical thickness of area posterior 24 in anterior cingulate and medial prefrontal cortex on migraine with aura. A. Leave-one-out plot. B. Forest plot. C. Scatter plot. D. Funnel plot.

**Supplementary Material 5: Figure S5.** MR plots for the causal effect of intracellular volume fraction of frontal opercular area 4 in insular and frontal opercular cortex on migraine with aura. A. Leave-one-out plot. B. Forest plot. C. Scatter plot. D. Funnel plot.

**Supplementary Material 6: Figure S6.** MR plots for the causal effect of intracellular volume fraction of area STSd anterior in auditory association cortex on migraine with aura. A. Leave-one-out plot. B. Forest plot. C. Scatter plot. D. Funnel plot.

**Supplementary Material 7: Figure S7.** MR plots for the causal effect of intrinsic curvature of area 9 Middle in anterior cingulate and medial prefrontal cortex on migraine without aura. A. Leave-one-out plot. B. Forest plot. C. Scatter plot. D. Funnel plot.

**Supplementary Material 8: Figure S8.** MR plots for the causal effect of local gyrification index of area TG dorsal in lateral temporal cortex on migraine without aura. A. Leave-one-out plot. B. Forest plot. C. Scatter plot. D. Funnel plot.

**Supplementary Material 9: Figure S9.** MR plots for the causal effect of orientation diffusion index of area IFSp in inferior frontal cortex on

migraine without aura. A. Leave-one-out plot. B. Forest plot. C. Scatter plot. D. Funnel plot.

**Supplementary Material 10: Figure S10.** MR plots for the causal effect of migraine with aura on the mean diffusivity of piriform cortex in insular and frontal opercular cortex. A. Leave-one-out plot. B. Forest plot. C. Scatter plot. D. Funnel plot.

**Supplementary Material 11:** Supplementary Tables.

**Supplementary Material 12:** Supplementary Text.

**Acknowledgements**
We sincerely appreciate the authors and participants of all the GWASs, including the Adolescent Brain Cognitive Development cohort, the UK Biobank cohort, the International Headache Genetics Consortium, and the Richard A. I. Bethlehem's group, from which we obtained GWAS summaries.

**Author contributions**
ZS, ML, GZ, NL, QS, and FL contributed to conception and design of the study. ZZ, JX, LS, and WZ performed the data preparation. ZS, ML, GZ, SW, and LJ conducted the statistical analysis. ML, ZS, QW, YW, and HW drew the figures. ZS, ML, GZ, and FL wrote the manuscript. All authors worked in the revision of the manuscript and approved the submitted version.

**Funding**
The present study was supported by the National Natural Science Foundation of China (82072001 and 82102133), the Beijing-Tianjin-Hebei Basic Research Collaboration Project (J230040), the Tianjin Natural Science Foundation (23JCZXJC00120), the Tianjin Key Medical Discipline (Specialty) Construction Project (TJYXZDXK-001 A), and the TianHe Qingsuo Open Research Fund of TSYS in 2022 & NSCCTJ (P-THQS-22-PY-No.0004).

**Data availability**
No datasets were generated or analysed during the current study.

## Declarations

**Ethics approval and consent to participate**
The participants' consents were obtained by the original studies.

**Consent for publication**
Not applicable.

**Competing interests**
The authors declare no competing interests.

**Author details**
[1]Department of Radiology, Tianjin Key Laboratory of Functional Imaging & Tianjin Institute of Radiology, Tianjin Medical University General Hospital, No. 154, Anshan Road, Heping District, Tianjin 300052, China
[2]Institute of Mental Health, Tianjin Anding Hospital, Mental Health Center of Tianjin Medical University, Tianjin 300222, China
[3]Brain Assessment & Intervention Laboratory, Tianjin Anding Hospital, Institute of Mental Health, Mental Health Center of Tianjin Medical University, Tianjin 300222, China
[4]Department of Molecular Imaging and Nuclear Medicine, Tianjin Medical University Cancer Institute and Hospital, National Clinical Research Center for Cancer, Tianjin Key Laboratory of Cancer Prevention and Therapy, Tianjin's Clinical Research Center for China, Tianjin 300060, China

Received: 19 September 2024 / Accepted: 23 October 2024
Published online: 28 October 2024

**References**

1. Gray PA, Burtness HI (1935) Hypoglycemic Headache*. Endocrinology 19:549–560. https://doi.org/10.1210/endo-19-5-549
2. Ferrari MD, Goadsby PJ, Burstein R, Kurth T, Ayata C, Charles A, Ashina M, van den Maagdenberg A, Dodick DW (2022) Migraine. Nat Rev Dis Primers 8:2. https://doi.org/10.1038/s41572-021-00328-4
3. Headache Classification Committee of the International Headache Society (IHS) (2018) The International classification of Headache disorders, 3rd edition. Cephalalgia 38(1–211). https://doi.org/10.1177/0333102417738202
4. Hansen JM, Charles A (2019) Differences in treatment response between migraine with aura and migraine without aura: lessons from clinical practice and RCTs. J Headache Pain 20:96. https://doi.org/10.1186/s10194-019-1046-4
5. Lucas C (2021) Migraine with aura. Rev Neurol (Paris) 177:779–784. https://doi.org/10.1016/j.neurol.2021.07.010
6. May A (2009) New insights into headache: an update on functional and structural imaging findings. Nat Rev Neurol 5:199–209. https://doi.org/10.1038/nrneurol.2009.28
7. Lerch JP, van der Kouwe AJ, Raznahan A, Paus T, Johansen-Berg H, Miller KL, Smith SM, Fischl B, Sotiropoulos SN (2017) Studying neuroanatomy using MRI. Nat Neurosci 20:314–326. https://doi.org/10.1038/nn.4501
8. Bashir A, Lipton RB, Ashina S, Ashina M (2013) Migraine and structural changes in the brain: a systematic review and meta-analysis. Neurology 81:1260–1268. https://doi.org/10.1212/WNL.0b013e3182a6cb32
9. Zhang X, Zhou J, Guo M, Cheng S, Chen Y, Jiang N, Li X, Hu S, Tian Z, Li Z, Zeng F (2023) A systematic review and meta-analysis of Voxel-based morphometric studies of migraine. J Neurol 270:152–170. https://doi.org/10.1007/s00415-022-11363-w
10. Messina R, Rocca MA, Goadsby PJ, Filippi M (2023) Insights into migraine attacks from neuroimaging. Lancet Neurol 22:834–846. https://doi.org/10.1016/S1474-4422(23)00152-7
11. Schwedt TJ, Chiang CC, Chong CD, Dodick DW (2015) Functional MRI of migraine. Lancet Neurol 14:81–91. https://doi.org/10.1016/S1474-4422(14)70193-0
12. Rahimi R, Dolatshahi M, Abbasi-Feijani F, Momtazmanesh S, Cattarinussi G, Aarabi MH, Pini L (2022) Microstructural white matter alterations associated with migraine headaches: a systematic review of diffusion tensor imaging studies. Brain Imaging Behav 16:2375–2401. https://doi.org/10.1007/s11682-022-00690-1
13. Valfre W, Rainero I, Bergui M, Pinessi L (2008) Voxel-based morphometry reveals gray matter abnormalities in migraine. Headache 48:109–117. https://doi.org/10.1111/j.1526-4610.2007.00723.x
14. Amin FM, De Icco R, Al-Karagholi MA, Raghava JM, Wolfram F, Larsson HBW, Ashina M (2021) Investigation of cortical thickness and volume during spontaneous attacks of migraine without aura: a 3-Tesla MRI study. J Headache Pain 22:98. https://doi.org/10.1186/s10194-021-01312-9
15. Guarnera A, Bottino F, Napolitano A, Sforza G, Cappa M, Chioma L, Pasquini L, Rossi-Espagnet MC, Lucignani G, Figa-Talamanca L, Carducci C, Ruscitto C, Valeriani M, Longo D, Papetti L (2021) Early alterations of cortical thickness and gyrification in migraine without aura: a retrospective MRI study in pediatric patients. J Headache Pain 22:79. https://doi.org/10.1186/s10194-021-01290-y
16. Komaromy H, He M, Perlaki G, Orsi G, Nagy SA, Bosnyak E, Kamson Olayinka D, John F, Trauninger A, Pfund Z (2019) Influence of hemispheric white matter lesions and migraine characteristics on cortical thickness and volume. J Headache Pain 20:4. https://doi.org/10.1186/s10194-019-0959-2
17. Arkink EB, Palm-Meinders IH, Koppen H, Milles J, van Lew B, Launer LJ, Hofman PAM, Terwindt GM, van Buchem MA, Ferrari MD, Kruit MC (2019) Microstructural white matter changes preceding white matter hyperintensities in migraine. Neurology 93:e688–e694. https://doi.org/10.1212/WNL.0000000000007940
18. Planchuelo-Gomez A, Garcia-Azorin D, Guerrero AL, Aja-Fernandez S, Rodriguez M, de Luis-Garcia R (2020) White matter changes in chronic and episodic migraine: a diffusion tensor imaging study. J Headache Pain 21:1. https://doi.org/10.1186/s10194-019-1071-3
19. Gomez-Beldarrain M, Oroz I, Zapirain BG, Ruanova BF, Fernandez YG, Cabrera A, Anton-Ladislao A, Aguirre-Larracoechea U, Garcia-Monco JC (2015) Right fronto-insular white matter tracts link cognitive reserve and pain in migraine patients. J Headache Pain 17:4. https://doi.org/10.1186/s10194-016-0593-1
20. Chong CD, Schwedt TJ (2015) Migraine affects white-matter tract integrity: a diffusion-tensor imaging study. Cephalalgia 35:1162–1171. https://doi.org/10.1177/0333102415573513
21. Huo J, Zhang G, Wang W, Cao W, Wan M, Huang T, Fan D, Fu Y (2023) Migraine and white matter lesions: a mendelian randomization study. Sci Rep 13:10984. https://doi.org/10.1038/s41598-023-38182-x

22. Sanderson E, Glymour MM, Holmes MV, Kang H, Morrison J, Munafo MR, Palmer T, Schooling CM, Wallace C, Zhao Q, Smith GD (2022) Mendelian randomization. Nat Rev Methods Primers 2. https://doi.org/10.1038/s43586-021-00092-5
23. Emdin CA, Khera AV, Kathiresan S (2017) Mendelian randomization. JAMA 318:1925–1926. https://doi.org/10.1001/jama.2017.17219
24. Guo X, Wang D, Ying C, Hong Y (2023) Association between brain structures and migraine: a bidirectional mendelian randomization study. Front Neurosci 17:1148458. https://doi.org/10.3389/fnins.2023.1148458
25. Zhao L, Zhao W, International Headache Genetics C, Cao J, Tu Y (2023) Causal relationships between migraine and microstructural white matter: a mendelian randomization study. J Headache Pain 24:10. https://doi.org/10.1186/s10194-023-01550-z
26. Warrier V, Stauffer EM, Huang QQ, Wigdor EM, Slob EAW, Seidlitz J, Ronan L, Valk SL, Mallard TT, Grotzinger AD, Romero-Garcia R, Baron-Cohen S, Geschwind DH, Lancaster MA, Murray GK, Gandal MJ, Alexander-Bloch A, Won H, Martin HC, Bullmore ET, Bethlehem RAI (2023) Genetic insights into human cortical organization and development through genome-wide analyses of 2,347 neuroimaging phenotypes. Nat Genet 55:1483–1493. https://doi.org/10.1038/s41588-023-01475-y
27. Gormley P, Anttila V, Winsvold BS, Palta P, Esko T, Pers TH, Farh KH, Cuenca-Leon E, Muona M, Furlotte NA, Kurth T, Ingason A, McMahon G, Ligthart L, Terwindt GM, Kallela M, Freilinger TM, Ran C, Gordon SG, Stam AH, Steinberg S, Borck G, Koiranen M, Quaye L, Adams HH, Lehtimaki T, Sarin AP, Wedenoja J, Hinds DA, Buring JE, Schurks M, Ridker PM, Hrafnsdottir MG, Stefansson H, Ring SM, Hottenga JJ, Penninx BW, Farkkila M, Artto V, Kaunisto M, Vepsalainen S, Malik R, Heath AC, Madden PA, Martin NG, Montgomery GW, Kurki MI, Kals M, Magi R, Parn K, Hamalainen E, Huang H, Byrnes AE, Franke L, Huang J, Stergiakouli E, Lee PH, Sandor C, Webber C, Cader Z, Muller-Myhsok B, Schreiber S, Meitinger T, Eriksson JG, Salomaa V, Heikkila K, Loehrer E, Uitterlinden AG, Hofman A, van Duijn CM, Cherkas L, Pedersen LM, Stubhaug A, Nielsen CS, Mannikko M, Mihailov E, Milani L, Gobel H, Esserlind AL, Christensen AF, Hansen TF, Werge T, International Headache, Genetics C, Kaprio J, Aromaa AJ, Raitakari O, Ikram MA, Spector T, Jarvelin MR, Metspalu A, Kubisch C, Strachan DP, Ferrari MD, Belin AC, Dichgans M, Wessman M, van den Maagdenberg AM, Zwart JA, Boomsma DI, Smith GD, Stefansson K, Eriksson N, Daly MJ, Neale BM, Olesen J, Chasman DI, Nyholt DR, Palotie A (2016) Meta-analysis of 375,000 individuals identifies 38 susceptibility loci for migraine. Nat Genet 48:856–866. https://doi.org/10.1038/ng.3598
28. Bulik-Sullivan B, Finucane HK, Anttila V, Gusev A, Day FR, Loh PR, ReproGen C, Psychiatric Genomics C, Genetic Consortium for Anorexia Nervosa of the Wellcome Trust Case, Control C, Duncan L, Perry JR, Patterson N, Robinson EB, Daly MJ, Price AL, Neale BM (2015) An atlas of genetic correlations across human diseases and traits. Nat Genet 47:1236–1241. https://doi.org/10.1038/ng.3406
29. Zanoaga MD, Friligkou E, He J, Pathak GA, Koller D, Cabrera-Mendoza B, Stein MB, Polimanti R (2024) Brainwide mendelian randomization study of anxiety disorders and symptoms. Biol Psychiatry 95:810–817. https://doi.org/10.1016/j.biopsych.2023.11.006
30. Zhao G, Lu Z, Sun Y, Kang Z, Feng X, Liao Y, Sun J, Zhang Y, Huang Y, Yue W (2023) Dissecting the causal association between social or physical inactivity and depression: a bidirectional two-sample mendelian randomization study. Transl Psychiatry 13:194. https://doi.org/10.1038/s41398-023-02492-5
31. Liu X, Tong X, Zou Y, Lin X, Zhao H, Tian L, Jie Z, Wang Q, Zhang Z, Lu H, Xiao L, Qiu X, Zi J, Wang R, Xu X, Yang H, Wang J, Zong Y, Liu W, Hou Y, Zhu S, Jia H, Zhang T (2022) Mendelian randomization analyses support causal relationships between blood metabolites and the gut microbiome. Nat Genet 54:52–61. https://doi.org/10.1038/s41588-021-00968-y
32. Hemani G, Tilling K, Davey Smith G (2017) Orienting the causal relationship between imprecisely measured traits using GWAS summary data. PLoS Genet 13:e1007081. https://doi.org/10.1371/journal.pgen.1007081
33. Burgess S, Thompson SG, Collaboration CCG (2011) Avoiding bias from weak instruments in mendelian randomization studies. Int J Epidemiol 40:755–764. https://doi.org/10.1093/ije/dyr036
34. Guo J, Yu K, Dong SS, Yao S, Rong Y, Wu H, Zhang K, Jiang F, Chen YX, Guo Y, Yang TL (2022) Mendelian randomization analyses support causal relationships between brain imaging-derived phenotypes and risk of psychiatric disorders. Nat Neurosci 25:1519–1527. https://doi.org/10.1038/s41593-022-01174-7
35. Burgess S, Davey Smith G, Davies NM, Dudbridge F, Gill D, Glymour MM, Hartwig FP, Kutalik Z, Holmes MV, Minelli C, Morrison JV, Pan W, Relton CL, Theodoratou E (2019) Guidelines for performing mendelian randomization investigations: update for summer 2023. Wellcome Open Res 4:186. https://doi.org/10.12688/wellcomeopenres.15555.3
36. Zhao QY, Wang JS, Hemani G, Bowden J, Small DS (2020) Ann Stat 48:1742–1769. https://doi.org/10.1214/19-Aos1866. Statistical Inference in Two-Sample Summary-Data Mendelian Randomization Using Robust Adjusted Profile Score
37. Greco MF, Minelli C, Sheehan NA, Thompson JR (2015) Detecting pleiotropy in mendelian randomisation studies with summary data and a continuous outcome. Stat Med 34:2926–2940. https://doi.org/10.1002/sim.6522
38. Ou Y, Ni X, Gao X, Yu Y, Zhang Y, Wang Y, Liu J, Yin Z, Rong J, Sun M, Chen J, Tang Z, Xiao W, Zhao L (2024) Structural and functional changes of anterior cingulate cortex subregions in migraine without aura: relationships with pain sensation and pain emotion. Cereb Cortex 34. https://doi.org/10.1093/cercor/bhae040
39. Xu WJ, Barisano G, Phung D, Chou B, Pinto SN, Lerner A, Sheikh-Bahaei N (2023) Structural MRI in migraine: a review of migraine vascular and structural changes in Brain Parenchyma. J Cent Nerv Syst Dis 15:11795735231167868. https://doi.org/10.1177/11795735231167868
40. Bliss TV, Collingridge GL, Kaang BK, Zhuo M (2016) Synaptic plasticity in the anterior cingulate cortex in acute and chronic pain. Nat Rev Neurosci 17:485–496. https://doi.org/10.1038/nrn.2016.68
41. Naylor B, Hesam-Shariati N, McAuley JH, Boag S, Newton-John T, Rae CD, Gustin SM (2019) Reduced glutamate in the Medial Prefrontal cortex is Associated with Emotional and Cognitive Dysregulation in People with Chronic Pain. Front Neurol 10:1110. https://doi.org/10.3389/fneur.2019.01110
42. Li XH, Matsuura T, Xue M, Chen QY, Liu RH, Lu JS, Shi W, Fan K, Zhou Z, Miao Z, Yang J, Wei S, Wei F, Chen T, Zhuo M (2021) Oxytocin in the anterior cingulate cortex attenuates neuropathic pain and emotional anxiety by inhibiting presynaptic long-term potentiation. Cell Rep 36:109411. https://doi.org/10.1016/j.celrep.2021.109411
43. Nagai M, Scheper V, Lenarz T, Forster CY (2021) The insular cortex as a vestibular area in relation to autonomic function. Clin Auton Res 31:179–185. https://doi.org/10.1007/s10286-020-00744-8
44. Zhang MM, Geng AQ, Chen K, Wang J, Wang P, Qiu XT, Gu JX, Fan HW, Zhu DY, Yang SM, Chen QY, Zhou ZX, Fan BY, Bai Y, Xing KK, Feng JM, Wang JD, Chen Y, Lu YC, Liang Y, Cao P, Kaang BK, Zhuo M, Li YQ, Chen T (2022) Glutamatergic synapses from the insular cortex to the basolateral amygdala encode observational pain. Neuron 110: 1993–2008 e1996. https://doi.org/10.1016/j.neuron.2022.03.030
45. Huang Y, Kakusa BW, Feng A, Gattas S, Shivacharan RS, Lee EB, Parker JJ, Kuijper FM, Barbosa DAN, Keller CJ, Bohon C, Mikhail A, Halpern CH (2021) The insulo-opercular cortex encodes food-specific content under controlled and naturalistic conditions. Nat Commun 12:3609. https://doi.org/10.1038/s41467-021-23885-4
46. Goadsby PJ, Holland PR, Martins-Oliveira M, Hoffmann J, Schankin C, Akerman S (2017) Pathophysiology of migraine: a disorder of sensory Processing. Physiol Rev 97:553–622. https://doi.org/10.1152/physrev.00034.2015
47. Arslan D, Unal Cevik I (2022) Interactions between the painful disorders and the autonomic nervous system. Agri 34:155–165. https://doi.org/10.14744/agri.2021.43078
48. Li Y, Li W, Zhang T, Zhang J, Jin Z, Li L (2021) Probing the role of the right inferior frontal gyrus during Pain-related empathy processing: evidence from fMRI and TMS. Hum Brain Mapp 42:1518–1531. https://doi.org/10.1002/hbm.25310
49. Ruland SH, Palomero-Gallagher N, Hoffstaedter F, Eickhoff SB, Mohlberg H, Amunts K (2022) The inferior frontal sulcus: cortical segregation, molecular architecture and function. Cortex 153:235–256. https://doi.org/10.1016/j.cortex.2022.03.019
50. Planchuelo-Gomez A, Garcia-Azorin D, Guerrero AL, Rodriguez M, Aja-Fernandez S, de Luis-Garcia R (2023) Structural brain changes in patients with persistent headache after COVID-19 resolution. J Neurol 270:13–31. https://doi.org/10.1007/s00415-022-11398-z
51. Stewart WF (1992) Prevalence of Migraine Headache in the United States. JAMA 267. https://doi.org/10.1001/jama.1992.03480010072027
52. Burch R, Rizzoli P, Loder E (2021) The prevalence and impact of migraine and severe headache in the United States: updated age, sex, and socioeconomic-specific estimates from government health surveys. Headache 61:60–68. https://doi.org/10.1111/head.14024
53. Avnon Y, Nitzan M, Sprecher E, Rogowski Z, Yarnitsky D (2004) Autonomic asymmetry in migraine: augmented parasympathetic activation in left unilateral migraineurs. Brain 127:2099–2108. https://doi.org/10.1093/brain/awh236

54. Kong XZ, Postema MC, Guadalupe T, de Kovel C, Boedhoe PSW, Hoogman M, Mathias SR, van Rooij D, Schijven D, Glahn DC, Medland SE, Jahanshad N, Thomopoulos SI, Turner JA, Buitelaar J, van Erp TGM, Franke B, Fisher SE, van den Heuvel OA, Schmaal L, Thompson PM, Francks C (2022) Mapping brain asymmetry in health and disease through the ENIGMA consortium. Hum Brain Mapp 43:167–181. https://doi.org/10.1002/hbm.25033
55. Wu J, Yang P, Wu X, Yu X, Zeng F, Wang H (2023) Association between second-hand smoke exposure and severe headaches or migraine in never-smoking adults. Headache 63:1341–1350. https://doi.org/10.1111/head.14640
56. Blaszczyk B, Straburzynski M, Wieckiewicz M, Budrewicz S, Niemiec P, Staszkiewicz M, Waliszewska-Prosol M (2023) Relationship between alcohol and primary headaches: a systematic review and meta-analysis. J Headache Pain 24:116. https://doi.org/10.1186/s10194-023-01653-7
57. Taschler B, Smith SM, Nichols TE (2022) Causal inference on neuroimaging data with mendelian randomisation. NeuroImage 258:119385. https://doi.org/10.1016/j.neuroimage.2022.119385

## Publisher's note